Journal of Power Sources 239 (2013) 490–495

Contents lists available at SciVerse ScienceDirect

Journal of Power Sources

journal homepage: www.elsevier.com/locate/jpowsour

Short communication

Improved electrochemical performance of $LiMO_2$ (M=Mn, Ni, Co)–Li_2MnO_3 cathode materials in ionic liquid-based electrolyte

Jie Li, Sangsik Jeong, Richard Kloepsch, Martin Winter, Stefano Passerini*

Institute of Physical Chemistry & MEET Battery Research Center, University of Muenster, Corrensstrasse 46, 48149 Muenster, Germany

HIGHLIGHTS

- High-voltage cathode material for high-energy Li-ion batteries.
- Ionic liquid based electrolytes lead to higher performance of cathode materials.
- Elevated temperature performance of $LiMO_2$–$LiMn_2O_3$ material.

ARTICLE INFO

Article history:
Received 24 September 2012
Received in revised form
10 January 2013
Accepted 5 April 2013
Available online 15 April 2013

Keywords:
Ionic liquid
Electrolyte
$LiMO_2$–Li_2MnO_3 cathode
Lithium batteries

ABSTRACT

Lithium bis(trifluoromethanesulfonyl)imide (LiTFSI) in *N*-butyl-*N*-methylpyrrolidinium bis(fluorosulfonyl) imide ($PYR_{14}FSI$) (1:9 in molar ratio) is successfully tested as electrolyte for the high voltage $LiMO_2$–Li_2MnO_3 (cathode)/lithium (anode) cells at elevated temperature (40 °C). Compared to conventional electrolytes, such as 1 M $LiPF_6$ solution in the mixed solvent of ethylene and dimethyl carbonate (EC:DMC = 1:1), the use of $PYR_{14}FSI$–LiTFSI electrolyte results in a net improvement of $LiMO_2$–Li_2MnO_3 cycling stability while granting comparable initial capacity. In addition, the ionic conductivity of the ionic liquid-based electrolyte at 40 °C is high enough to sustain the excellent rate capability of this cathode material. Li/$LiMO_2$–Li_2MnO_3 cells delivered initial capacity exceeding 200 mA h g^{-1} at high current rate (2 C) while retaining 94% of the initial capacity after 100 cycles. Differential capacity versus potential analysis and post-mortem characterization by scanning electron microscope, X-ray diffraction and were carried out to explain the improved performance of $LiMO_2$–Li_2MnO_3 in the IL-based electrolyte.

1. Introduction

The challenges for rechargeable batteries are considered to be cost, safety, energy, power and life [1]. Thus, the identification of cheaper, higher capacity and safer cathode materials has attracted much attention in the field of lithium ion battery research. In this regard, solid solutions of layered Li_2MnO_3 and $LiMO_2$ (M = Mn, Co, Ni, etc.) have been proved to be promising candidates for cathode materials. Considering its high capacity, over 250 mA h g^{-1} as the initial capacity, improved safety, the high Mn content, granting better thermal stability than $Li(Ni_{0.33}Mn_{0.33}Co_{0.33})O_2$, and low cost, low Ni and Co content, this material fulfills the requirements for next-generation cathode materials [2–5].

Charging $LiMO_2$–Li_2MnO_3 to high potential, typically 4.6–4.8 V vs Li/Li^+, lithium can be extracted from the "inert" Li_2MnO_3 rock-salt phase, which involves a contemporaneous release of oxygen, therefore enhancing the discharge capacity [6,7]. In our previous work, the electrochemical performance at 20 °C was already extensively investigated [8,9]. Based on these results, it is noticeable as this material is quite sensitive to the temperature. A slight temperature change from 20 °C to 25 °C [9] leads to an obvious capacity increase at both low and high current rate.

As mentioned earlier, in order to access the high capacity of $LiMO_2$–Li_2MnO_3, the composite cathode electrodes must be charged to high voltage to activate the Li_2MnO_3 component [10]. However, in today's market, the majority of Li-ion batteries use organic carbonate-based electrolytes, which decompose above 4.5 V vs Li/Li^+ [11,12]. Thus, the required upper cutoff voltage for this cathode material (as high as 4.8 V) is well beyond the electrochemical stability window of the conventional electrolyte, such as 1 M $LiPF_6$ in ethylene carbonate (EC):dimethyl carbonate (DMC) (1:1 vol) solution, especially at temperatures above room temperature. The decomposition products from the electrolyte may deposit on the cathode surface as a thick solid interphase, leading to irreversibility of the lithium intercalation/de-intercalation process

* Corresponding author.
E-mail address: Stefano.passerini@uni-muenster.de (S. Passerini).

0378-7753/$ – see front matter © 2013 Elsevier B.V. All rights reserved.
http://dx.doi.org/10.1016/j.jpowsour.2013.04.015

and cell degradation. The oxidation of carbonate solvent at high voltages also generates gases, which results in an increase of the internal battery pressure, eventually resulting in battery failure. Meanwhile, the conventional carbonate electrolytes are volatile and flammable, causing serious safety problems, especially at elevated temperature. Thus, identifying alternative electrolytes with wider electrochemical stability window and better thermal stability is a very efficient method to improve the $LiMO_2$–Li_2MnO_3 cathode based cells.

Recently, ionic liquids (ILs) are being considered as electrolyte components for lithium and lithium-ion batteries. Their good electrochemical stability, low volatility and flammability compared to the organic carbonates currently used in lithium-ion batteries [13,14], may result in improved stability performance at elevated temperature, which would match the $LiMO_2$–Li_2MnO_3 cathode material very well. One of the most popular ionic liquids reported as promising electrolyte component for lithium-ion batteries, is *N*-butyl-*N*-methylpyrrolidinium bis(trifluoromethanesulfonyl)imide ($PYR_{14}TFSI$). Its incorporation into polymer electrolytes is widely reported in lithium battery system [15–17]. However, low ionic conductivity and high viscosity limit its application in combination with high power cathode materials. Because of this, *N*-butyl-*N*-methylpyrrolidinium bis(fluorosulfonyl)imide ($PYR_{14}FSI$), characterized by lower melting point and viscosity and comparable electrochemical stability window versus $PYR_{14}TFSI$-based electrolyte [13,18], is being considered. Additionally, this ionic liquid is thermally stable up to 125 °C. These properties altogether make $PYR_{14}FSI$ as a very promising electrolyte solvent for high rate, high voltage lithium batteries, as those comprising $LiMO_2$–Li_2MnO_3 cathodes.

In this work, the investigations of the electrochemical behavior of $0.4LiMn_{0.4}Ni_{0.4}Co_{0.2}O_2$–$0.6Li_2MnO_3$ (or $Li[Li_{0.2}Mn_{0.56}Ni_{0.16}Co_{0.08}]O_2$) cathode material with $PYR_{14}FSI$ based electrolyte is reported, especially at elevated temperature (40 °C). Lithium bis(trifluoromethanesulfonyl)imide (LiTFSI) is used as lithium salt because of its higher thermal stability than $LiPF_6$. In order to compare the results, all tests were also carried out on cells using an organic carbonate-based electrolyte (1 M $LiPF_6$ in EC/DMC).

2. Experimental part

$Li[Li_{0.2}Mn_{0.56}Ni_{0.16}Co_{0.08}]O_2$, a composition of $LiMO_2$ and Li_2MnO_3 with 4:6 M ratio, was synthesized by a solid-state reaction method from lithium hydroxide hydrate (Aldrich >98%) and manganese–nickel–cobalt hydroxide precursors following a previously published method [9].

$PYR_{14}FSI$ was synthesized through a procedure developed at ENEA [19]. LiTFSI (99.9 wt %, battery grade) was purchased from 3 M (USA). It was dried at 100 °C under turbomolecular pump vacuum prior to use. $Pyr_{14}FSI$/LiTFSI electrolyte was made dissolving the appropriate amount of lithium salt in the ionic liquid.

Electrodes were prepared by casting slurries with composition of 85 wt.% active material, 10 wt.% Super C65 (TIMCAL), and 5 wt.% PVDF binder (Kynar® FLEX 2801, Arkema Group) onto an aluminum current collector foil. The electrode tapes were punched to 12 mm discs and dried at 120 °C under vacuum for 24 h. The mass loading of active material was about 2 mg cm^{-2}. The electrodes were assembled into pouch cells using 1 M $LiPF_6$ in EC + DMC solution or $PYR_{14}FSI$/LiTFSI as the electrolyte. Metallic lithium foil was used for both the counter and reference electrodes. Glass fiber (Whatman) was used as separator. Vacuum was applied for 30 min prior sealing the cells in order to secure the wetting of the separator and electrode.

The electrochemical performance of the cells was tested with Maccor series 4000 battery tester. The cells were stored in climatic chambers, which temperature was fixed at 40 °C (±1 °C). Cells with different electrolytes are compared by their cycling performance at 0.5 C (nominal capacity = 200 mA h g^{-1}, 1 C = 200 mA g^{-1}). Rate tests were carried out continuously cycling the cells at various rates (0.2 C, 0.5 C, 1 C, 2 C and 5 C).

For post-mortem characterization, the cycled pouch cells were opened in a dry room (dew point < −60 °C). The cathode electrodes were removed and thoroughly rinsed with DMC to remove all electrolyte components. The crystalline structure of cycled electrodes was characterized by X-ray diffraction (XRD) using the Cu Kα radiation on the Bruker D8 Advance (Germany) in the 2θ range from 10° to 90°. The electrode morphology was characterized by high resolution scanning electron microscopy (SEM, AURIGA® microscope, Zeiss).

3. Results and discussion

To show the effect of temperature on the performance of $Li[Li_{0.2}Mn_{0.56}Ni_{0.16}Co_{0.08}]O_2$, electrodes comprising it were cycled in 1 M $LiPF_6$ in EC/DMC electrolyte at different temperatures. Fig. 1 shows the comparison of cycling performance for two cells, which were cycled between 2.5 V and 4.8 V and C/2 rate at 20 °C and 40 °C. It can be seen that the electrochemical performance of this material is very sensitive to the temperature. At 40 °C, the material delivered an initial capacity of 286 mA h g^{-1}, which is substantially higher than that obtained at 20 °C (234 mA h g^{-1}). However, the capacity fading upon cycling is also much higher at elevated temperature. Only 54% of the initial material capacity was retained after 100 cycles at 40 °C, while a value reaching 78% was observed at 20 °C.

The main reason for this fading may originate from electrolyte decomposition. It is well-known that conventional organic electrolytes undergo electrochemical oxidation at high working potential and elevated temperature [20–22]. The decomposition of electrolyte may consume active lithium, plate highly resistive products on the electrode surface, cause cathode self-discharge, and generate gases. All these may affect the active material capacity fading excluding the internal cell pressure increase, which, on the other hand, may raise safety issues.

In order to improve the electrochemical performance of $Li[Li_{0.2}Mn_{0.56}Ni_{0.16}Co_{0.08}]O_2$ at elevated temperature, the replacement of the conventional electrolyte with a more stable system, for

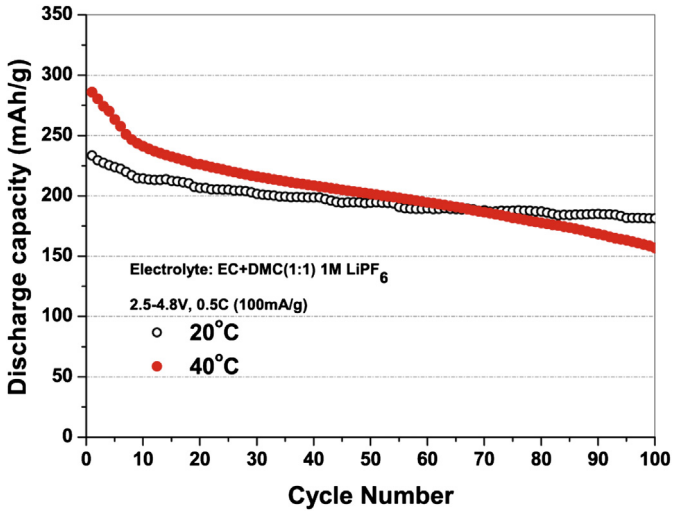

Fig. 1. Comparison of cycling performance of $Li[Li_{0.2}Mn_{0.56}Ni_{0.16}Co_{0.08}]O_2$ electrodes with 1 M $LiPF_6$ EC/DMC electrolyte. Cutoff voltages: 2.5 V and 4.8 V. C rate: 0.5 C.

instance an electrolyte based on non volatile, thermally stable ionic liquids, appears to be a promising way. Fig. 2 shows the long-term cycling performance of $Li[Li_{0.2}Mn_{0.56}Ni_{0.16}Co_{0.08}]O_2$ electrodes in $PYR_{14}FSI$/LiTFSI (9:1 M ratio) electrolyte at 0.5 C and 40 °C. For comparison purposes, the same test was also carried out with 1 M $LiPF_6$ in EC/DMC as electrolyte. Independent on the voltage range used, the electrodes tested in combination with the IL-based electrolyte showed an obviously better cycling stability. The material delivered 287 mA h g^{-1} (Fig. 2a) initial capacity within the voltage range of 2.5–4.8 V, with a capacity retention of 78% after 100 cycles (final capacity of 225 mA h g^{-1}) while the coulombic efficiency reached 99.5% after a few initial cycles. On the contrary, the electrode in combination with the conventional electrolyte showed much worse cycling stability and lower coulombic efficiency (always below 98%). Additionally, the capacity fading tends to progressively increase upon cycling. This poor performance is certainly due to the electrolyte decomposition occurring at high potential and temperature, even though some active material degradation must also occur to explain the higher capacity fading over cycling. However, both reactions do not take place in presence of the IL-based electrolyte. Because of its better stability at both high voltage and temperature, the cathode material shows better cycling performance. It is worth mentioning that, independent of the electrolyte used, both cells delivered the same initial capacity, which implies the conductivity of $PYR_{14}FSI$/LiTFSI at 40 °C sufficient to warrant the cell operation at 0.5 C rate.

Decreasing the cell cutoff voltage to 4.6 V results in the improved cycling stability of cells employing both electrolytes due to lower irreversible reaction at the electrolyte/cathode interface. Nevertheless, the cell employing the IL-based electrolyte still showed lower capacity fading with 84% retention after 100 cycles while the initial capacity (about 255 mA h g^{-1}) was similar to that obtained with the conventional electrolyte. Thus, it can be concluded that use $PYR_{14}FSI$/LiTFSI as electrolyte can significantly improve the cycling stability of $Li[Li_{0.2}Mn_{0.56}Ni_{0.16}Co_{0.08}]O_2$ at the investigated temperature.

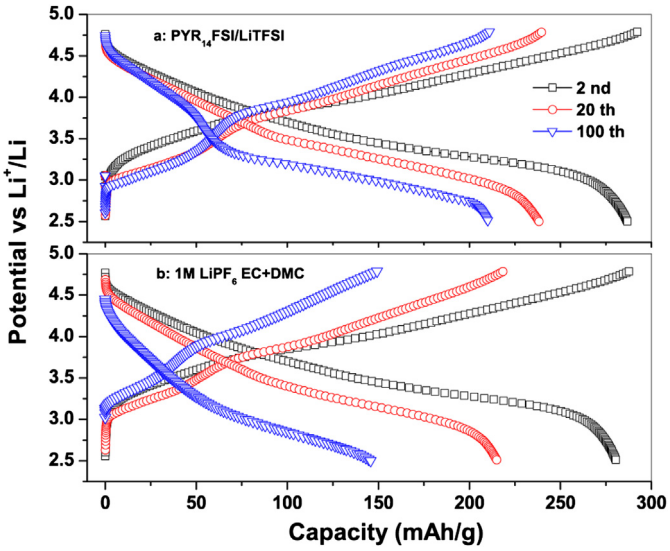

Fig. 3. Voltage profiles of $Li[Li_{0.2}Mn_{0.56}Ni_{0.16}Co_{0.08}]O_2$ electrodes with (a) $PYR_{14}FSI$/LiTFSI and (b) 1 M $LiPF_6$ EC + DMC electrolytes detected during cycle tests at 0.5 C and 40 °C within 2.5 V and 4.8 V cutoff limits.

To clarify the improved long-term cycling performance of $Li[Li_{0.2}Mn_{0.56}Ni_{0.16}Co_{0.08}]O_2$ in the IL-based electrolyte, the changes occurring during the lithium intercalation and deintercalation processes were considered. Fig. 3 shows the 2nd, 20th, and 100th potential profiles of the electrodes with the two different electrolytes. The 2nd cycle profiles in Fig. 3a (IL-based electrolyte) and Fig. 3b (1 M $LiPF_6$ EC + DMC electrolyte) appear very similar in shape, showing a continuous change of potential during both charge and discharge steps. However, upon further cycling, a split into two regions (sloping plateaus), from 4.8 to 3.5 V and 3.5 to 2.5 V, separated by a marked potential change is observed (see the 20th cycle discharge curves in both Fig. 3a and b). Interestingly, as it

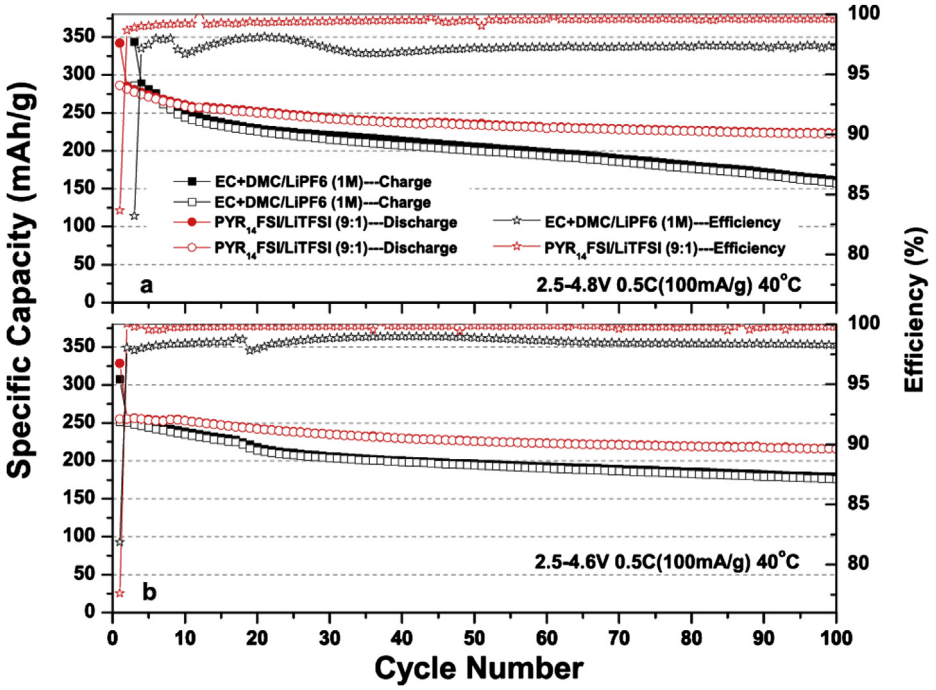

Fig. 2. The comparison of cycling performance of $Li[Li_{0.2}Mn_{0.56}Ni_{0.16}Co_{0.08}]O_2$ electrodes cycled at 0.5 C and 40 °C with different electrolytes and cutoff voltages. See insets for details.

can be seen in the 100th cycle discharge curves, the two-plateau feature was maintained in the cell with the IL-based electrolyte, while it disappeared in that with the conventional electrolyte.

The low voltage plateau occurring at 3.5–2.5 V is typical for the second lithium intercalation in the spinel phase [23]. Its appearance indicates that the layered structure of $Li[Li_{0.2}Mn_{0.56}Ni_{0.16}Co_{0.08}]O_2$ may convert to spinel phase during the cycling. This is not unexpected in such a high manganese content, layered material, and was already discussed in previous work of other groups [24,25]. Post-mortem XRD measurements were performed on the cycled electrodes to confirm the phase transformation occurring in the material upon long-term cycling tests (100 cycles). The resulting XRD patterns are compared with that of the pristine material in Fig. 4. As it can be seen in the figure, the patterns of the cycled electrodes show lower and broader peaks, indicating that the crystallinity of the material decreases after long-term cycling. The position of (104), (006) and (102) shift to lower 2θ due to the lattice expansion along the *c* axis [26] as a result of a lowered lithium content in the layered structure. However, a new peak at 38.6° is observed in the cycled electrodes, which can be assigned to the (222) diffraction of spinel structure. This confirms that the proposed phase transformation from layered to spinel takes place during the long-term cycling test. During the electrochemical processes the material experience the intergrowth of layer-spinel structure.

However, it has to be mentioned that even though the IL-based electrolyte can significantly improve the capacity retention of Li-rich material, the working voltage plateau of the latter fades upon cycling. It is obvious that the energy of the cell will continuously decrease on cycling, which is considered to be the main defect of this cathode material, in general. Further improvements of the material are needed before its practical use.

To further clarify this issue, derivative capacity vs voltage (*dQ*/*dV*) plots are graphed in Fig. 5. During the first charge process, in both graphs a strong peak above 4.5 V, which arises from the electrochemical activation of the Li_2MnO_3 component accompanied by oxygen loss, is observed. In the following cycles, however, some differences can be observed. The first one is observed in the region extending from 3.0 V to 4.0 V, especially during the discharge process, which corresponds to the lithium insertion/extraction reactions from the octahedral sites of the layered

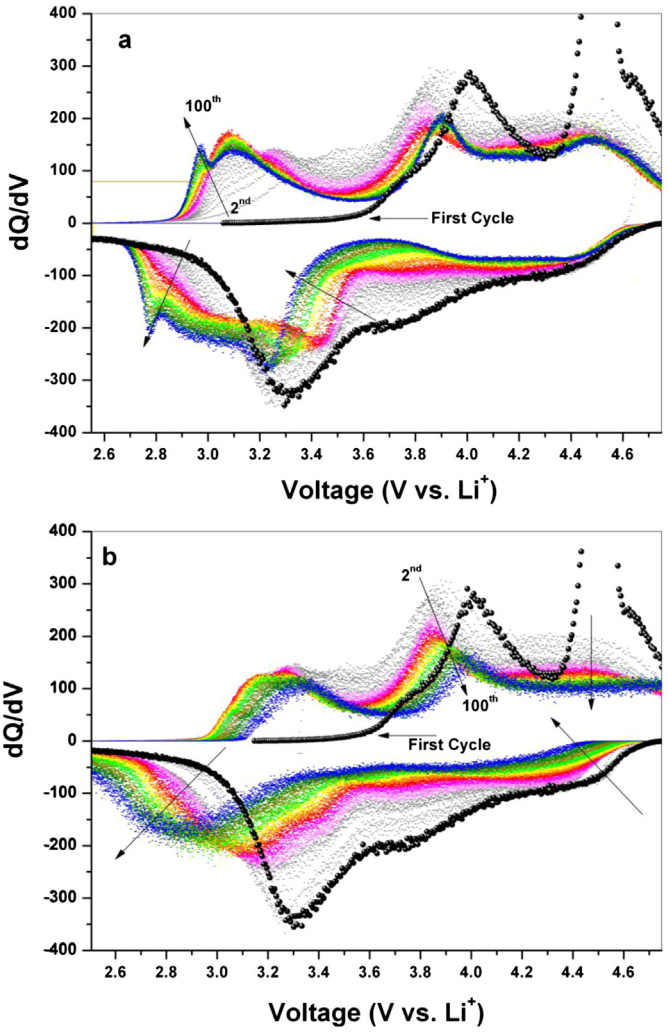

Fig. 5. Evolution of *dQ*/*dV* versus potential of $Li[Li_{0.2}Mn_{0.56}Ni_{0.16}Co_{0.08}]O_2$ electrodes cycled in (a) $PYR_{14}FSI$/LiTFSI and (b) 1 M $LiPF_6$ EC + DMC electrolytes at 0.5 C and 40 °C within 2.5 V and 4.8 V cutoff limits. The first cycle is evidenced by larger markers.

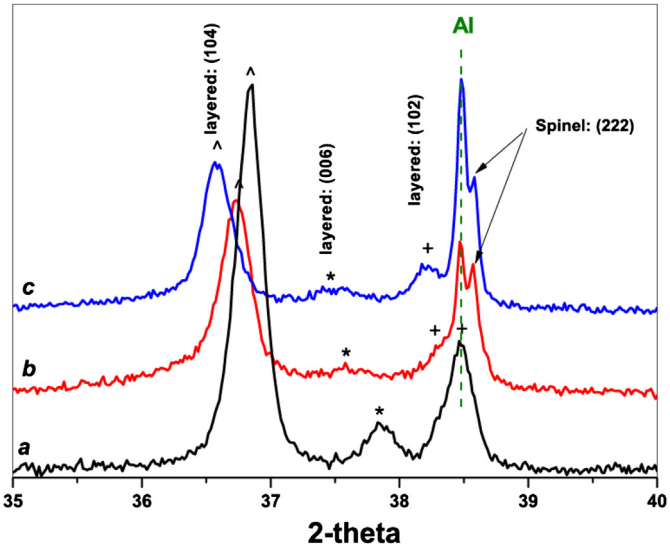

Fig. 4. XRD patterns of $Li[Li_{0.2}Mn_{0.56}Ni_{0.16}Co_{0.08}]O_2$ taken from a) pristine powder and electrodes cycled at 0.5 C and 40 °C within 2.5 V and 4.8 V cutoff limits in b) $PYR_{14}FSI$/LiTFSI or c) 1 M $LiPF_6$ EC + DMC electrolyte.

structure. With both electrolytes a shift toward lower voltage and an intensity decrease of the main peak is observed, which is, however, much more marked in presence of the conventional electrolyte. Secondly, an intensity decrease is also observed for the redox features above 4.2 V, corresponding to the lithium insertion/extraction from the tetrahedral sites [25]. After initial 10 cycles, these features disappear completely in the cell using the conventional electrolyte while they reached a steady state in that with the IL-based electrolyte. Finally, a sharp new redox peak couple emerges at about 2.7–3.0 V during cycling, which is typical of the second lithium ion intercalation into the spinel structure, which confirms the evolution of this new phase upon cycling. This feature is almost not seen in the *dQ*/*dV* curve of the cell with conventional electrolyte, confirming that the spinel phase is electrochemical activity only in the cell with the IL-based electrolyte.

In the cell with conventional electrolyte, the newly formed spinel phase suffers the well-known inconvenient of manganese dissolution into the electrolyte, occurring, especially at high temperature, as a result of the Jahn–Teller distortion [23]. This is known to lead to serious capacity fading upon long-term cycling of spinel $LiMn_2O_4$.

Among the reason for the improved behavior of the material in IL-based electrolytes, a low solubility of manganese ions in the IL

might be the reason for the stability of the evolving spinel phase and, thus, the reversibility of the whole electrochemical process. Although further measurements are needed to confirm the proposed lower solubility of divalent manganese, e.g., the determination of dissolved manganese in the few microliters of electrolyte present in the cells, it is appears reasonable to explain the better cycling performance of the material in IL-based electrolyte at elevated temperature.

Beside the active material, the stability of the electrolyte itself also needs to be considered since the decomposition of conventional electrolyte at high temperature may introduce high resistance into the cell. Thus, it is worthwhile to investigate the changes taking place on the electrode surface upon cycling, due to electrolyte decomposition. The surface morphology of cycled Li[$Li_{0.2}Mn_{0.56}Ni_{0.16}Co_{0.08}$]$O_2$ electrodes is shown in Fig. 6 where are illustrated the SEM images of electrodes after 100 cycles with either PYR14FSI/LiTFSI (9:1) (Fig. 6a) or 1 M $LiPF_6$ EC + DMC (Fig. 6b) electrolyte. The electrode cycled in ILs electrolyte shows much cleaner particle surfaces compared to those of the electrode cycled in organic electrolyte. In the latter, it can be observed that some compounds have been generated on the surface of the electrode (highlighted with circles), which may originate from electrolyte decomposition. These compounds plate on the electrode surface, preventing a good interface with the electrolyte and, then,

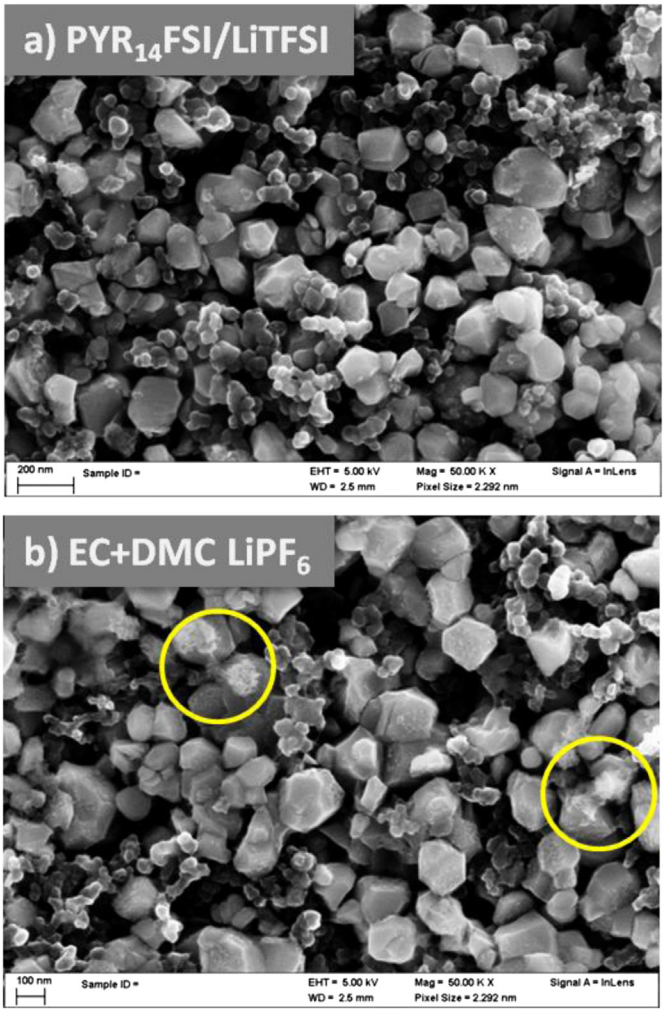

Fig. 6. SEM images of cycled Li[$Li_{0.2}Mn_{0.56}Ni_{0.16}Co_{0.08}$]$O_2$ electrodes in (a) PYR_{14}FSI/LiTFSI and (b) 1 M $LiPF_6$ EC + DMC electrolyte.

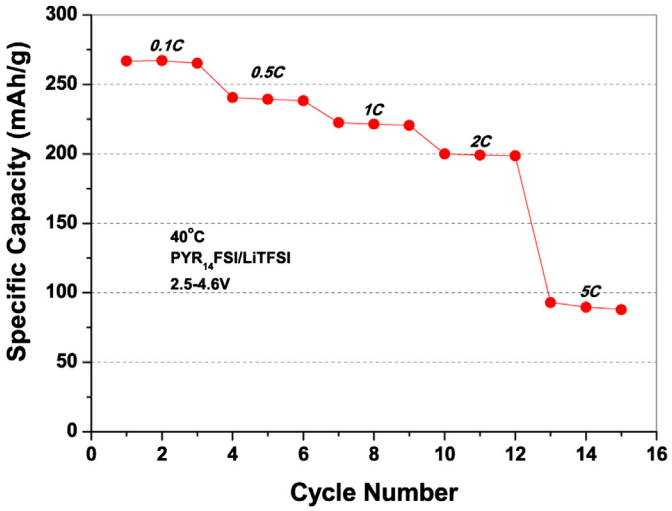

Fig. 7. Rate performance of Li[$Li_{0.2}Mn_{0.56}Ni_{0.16}Co_{0.08}$]$O_2$ electrodes in PYR_{14}FSI/LiTFSI electrolyte cycled at 40 °C within 2.5 V and 4.6 V cutoff limits.

increasing the cell resistance. This increasing internal resistance may also contribute to the faster increasing potential drop observed in the cell with conventional electrolyte (see Fig. 3). The absence of reaction products in the electrode cycled in PYR_{14}FSI/LiTFSI (9:1) supports for its stability in contact with high-voltage cathode materials and as a promising candidate for the realization of high voltage lithium batteries, especially those operating at elevated temperatures.

Finally, the rate test of Li[$Li_{0.2}Mn_{0.56}Ni_{0.16}Co_{0.08}$]$O_2$ electrodes in PYR_{14}FSI/LiTFSI (9:1) electrolyte at 40 °C was carried out, which results are shown in Fig. 7. The test was performed using the cutoff limits of 2.5 V and 4.6 V. In this voltage range, the material still exhibits a capacity of ~270 mA h g^{-1} at 0.1 C without fading. The discharge capacity reached 240 mA h g^{-1}, 220 mA h g^{-1} and 200 mA h g^{-1} at 0.5 C, 1 C and 2 C, respectively. However, during the 5 C rate test the capacity decreased abruptly to less than 90 mA h g^{-1}. Nevertheless, the performance offered by the cell employing the IL-based electrolyte up to 2 C rate is extremely good, to the best of our knowledge such a good performance was never reported in IL-based electrolytes, and certainly interesting for practical applications.

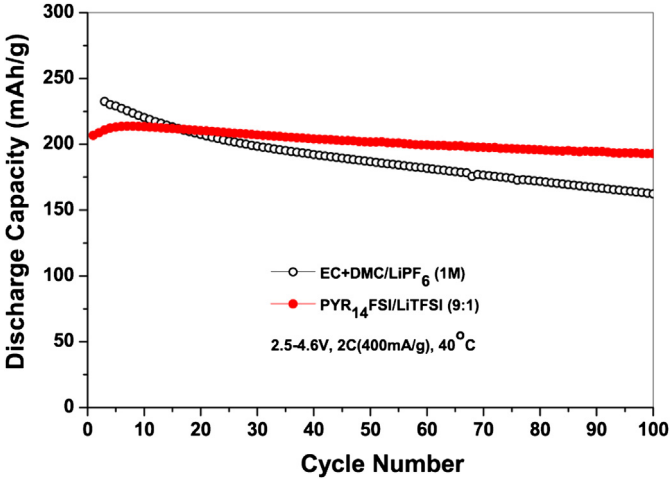

Fig. 8. Comparison of cycling performance of Li[$Li_{0.2}Mn_{0.56}Ni_{0.16}Co_{0.08}$]$O_2$ electrodes cycled in different electrolytes at 2 C rate and 40 °C within 2.5 V and 4.6 V cutoff limits.

On the basis of the rate test results, a long-term cycling performance test of $Li[Li_{0.2}Mn_{0.56}Ni_{0.16}Co_{0.08}]O_2$ was performed at 2 C (Fig. 8). As expected, the cell employing the IL-based electrolyte showed better cycling stability than that using the conventional electrolyte. It delivered an initial capacity of 206 mA h g^{-1}, which only slightly decreased to 193 mA h g^{-1} (94%) after 100 cycles. On the other hand, the cell with the conventional electrolyte showed a severe capacity fading although its initial capacity was higher.

4. Conclusion

The use of $PYR_{14}FSI$/LiTFSI (9:1) as an electrolyte for Li_2MnO_3–$LiMO_2$ high voltage cathode materials appears to be very promising, especially at elevated temperature. In fact, it has been proved that, at 40 °C, $Li[Li_{0.2}Mn_{0.56}Ni_{0.16}Co_{0.08}]O_2$ electrodes can perform similar initial capacity and much better cycling stability compared to those cycled in a conventional electrolyte. It exhibits a first discharge capacity of 286 mA h g^{-1} with retention of 78% after 100 cycles. Even upon a charge/discharge test at high current rate (2 C), the material delivered over 200 mA h g^{-1} in the first cycle with a capacity retention of 94% after 100 cycles. In simpler words, using $PYR_{14}FSI$/LiTFSI (9:1) as the electrolyte allows the high-voltage cathode to show excellent performance in terms of capacity, rate capability and long-term cycle stability.

These improvements originate from the ionic liquids high stability at elevated temperature and operating potential and, most probably, the low manganese solubility in these electrolytes, which prevents the dissolution of the spinel phase evolving upon cycling.

Acknowledgments

The authors kindly acknowledge the financial support from Federal Ministry of Education and Research (BMBF), Federal Ministry of Economic and Technology (BMWi) and Federal Ministry for the Environment, Nature Conservation and Nuclear Safety (BMU) within the project KaLiPat and European Commission within the FP7 Project LABOHR (FP7-2010-GC-Electrochemical–Storage 265971) RK kindly acknowledges “Hans-L.-Merkle Stiftung” for financial support.

References

[1] J.B. Goodenough, Journal of Solid State Electrochemistry 16 (6) (2012) 2019–2029.
[2] Y.S. Hong, et al., Journal of Materials Chemistry 14 (9) (2004) 1424–1429.
[3] K. Jeom-Soo, et al., Chemistry of Materials 16 (10) (2004).
[4] C.S. Johnson, et al., Electrochemistry Communications 6 (10) (2004) 1085–1091.
[5] M.M. Thackeray, et al., Journal of Materials Chemistry 15 (23) (2005) 2257–2267.
[6] A.R. Armstrong, A.D. Robertson, P.G. Bruce, Journal of Power Sources 146 (1–2) (2005) 275–280.
[7] A.R. Armstrong, et al., Journal of the American Chemical Society 128 (26) (2006) 8694–8698.
[8] J. Li, et al., Journal of Power Sources 196 (18) (2011) 7687–7691.
[9] J. Li, et al., Journal of Power Sources 196 (10) (2011) 4821–4825.
[10] J. Zheng, et al., Electrochimica Acta 59 (2012) 14–22.
[11] L. Yang, B. Ravdel, B.L. Lucht, Electrochemical and Solid State Letters 13 (8) (2010) A95–A97.
[12] A. von Cresce, K. Xu, Journal of the Electrochemical Society 158 (3) (2011) A337–A342.
[13] E. Paillard, et al., Journal of the Electrochemical Society 156 (11) (2009) A891–A895.
[14] M. Kunze, et al., Advanced Energy Materials 1 (2) (2011) 274–281.
[15] J.H. Shin, et al., Journal of the Electrochemical Society 153 (9) (2006) A1649–A1654.
[16] J. Rymarczyk, et al., European Polymer Journal 44 (7) (2008) 2153–2161.
[17] G.B. Appetecchi, et al., Journal of Power Sources 195 (11) (2010) 3668–3675.
[18] Q. Zhou, et al., Journal of Physical Chemistry B 112 (43) (2008) 13577–13580.
[19] G.B. Appetecchi, et al., Journal of the Electrochemical Society 153 (9) (2006) A1685–A1691.
[20] K. Xu, Chemical Reviews 104 (10) (2004) 4303–4417.
[21] J. Li, et al., Journal of Physical Chemistry C 112 (32) (2008) 12550–12556.
[22] S.E. Sloop, et al., Electrochemical and Solid State Letters 4 (4) (2001) A42–A44.
[23] M.M. Thackeray, Progress in Solid State Chemistry 25 (1–2) (1997) 1–71.
[24] S.K. Martha, et al., Journal of Power Sources 199 (2012) 220–226.
[25] C.S. Johnson, et al., Chemistry of Materials 20 (19) (2008) 6095–6106.
[26] J. Li, et al., Solid State Ionics 177 (17–18) (2006) 1509–1516.